Behavioral/Systems/Cognitive

A Circuit Model for Saccadic Suppression in the Superior Colliculus

Penphimon Phongphanphanee,[1]* Fengxia Mizuno,[2]* Psyche H. Lee,[2] Yuchio Yanagawa,[3,4] Tadashi Isa,[1] and William C. Hall[2]

[1]National Institute for Physiological Sciences, Okazaki 444-8585, Japan, [2]Department of Neurobiology, Duke University Medical Center, Durham, North Carolina 27710, [3]Department of Genetics and Behavioral Neuroscience, Gunma University Graduate School of Medicine, Maebashi 371-8511, Japan, and [4]Japan Science and Technology Agency, Core Research for Evolutional Science and Technology, Tokyo 107-0075, Japan

Attenuation of visual activity in the superficial layers (SLs), stratum griseum superficiale and stratum opticum, of the superior colliculus during saccades may contribute to reducing perceptual blur during saccades and also may help prevent subsequent unwanted saccades. GABAergic neurons in the intermediate, premotor, layer (SGI), stratum griseum intermedium, send an inhibitory input to SL. This pathway provided the basis for a model proposing that the SGI premotor cells that project to brainstem gaze centers and discharge before saccades also activate neighboring GABAergic neurons that suppress saccade-induced visual activity in SL.

The *in vitro* method allowed us to test this model. We made whole-cell patch-clamp recordings in collicular slices from either rats or GAD67–GFP knock-in mice, in which GABAergic neurons could be identified by their expression of green fluorescence protein (GFP). Antidromic electrical stimulation of SGI premotor cells was produced by applying pulse currents in which their axons congregate after exiting the superior colliculus. The stimulation evoked monosynaptic EPSCs in SGI GABAergic neurons that project to SL, as would be predicted if these neurons receive excitatory input from the premotor cells. Second, IPSCs were evoked in SL neurons, some of which project to the visual thalamus. These IPSCs were polysynaptically mediated by the GABAergic neurons that were excited by the antidromically activated SGI neurons. These results support the hypothesis that collaterals of premotor neuron axons excite GABAergic neurons that inhibit SL visuosensory cells.

Introduction

As the eyes move during a shift in the direction of gaze, the optical projection of the visual field sweeps across the retina at the same speed in the opposite direction, but the resulting retinal stimulation does not result in either the perception of visual motion during the eye movement or the triggering of subsequent, unwanted shifts in gaze (Volkmann, 1962).

A circuit model to explain the suppression of the visual activity evoked by saccades proposes that premotor neurons in the intermediate layers of the superior colliculus that initiate saccades have corollary discharges that suppress the visual activity in the superficial layers (SL) (see Fig. 1). Two types of *in vitro* experiments suggested that this circuitry is located within the superior colliculus (Lee et al., 2007). First, in GAD67–GFP knock-in mice, in which GABAergic neurons express green fluorescent protein (GFP) (Tamamaki et al., 2003), GFP-labeled SGI neurons were injected with the axonal tracer biocytin. The results revealed a population of SGI GABAergic neurons that project to SL. Second, whole-cell patch-clamp recordings of cells in SL were obtained from both rats and mice. The recordings detected large IPSCs in SL cells evoked by stimulation in SGI. These IPSCs were monosynaptic and blocked by GABAzine, confirming that they are $GABA_A$ receptor-mediated IPSCs.

In the present experiments, we tested this model by measuring the responses of both SGI GABAergic and SL projection cells evoked by antidromically stimulating the axons of SGI cells that exit the superior colliculus. Many of these SGI efferent cells project to the brainstem gaze centers that organize and initiate shifts in the direction of gaze (Harting et al., 1973; Moschovakis et al., 1988a,b; May, 2006). These experiments provide direct evidence for the model by demonstrating that the activation of SGI efferent axons can induce polysynaptic IPSCs in SL neurons that project to the visual thalamus.

Materials and Methods

The experimental design was to whole-cell patch-clamp record *in vitro* the responses of SGI and SL cells to antidromic stimulation of premotor cells (Fig. 1).

Preparation of slices. Procedures for slice preparation were described in previous reports (Lee and Hall, 1995; Phongphanphanee et al., 2008). Briefly, coronal slices (250–300 μm thick) of the superior colliculus were prepared from Sprague Dawley rats, C57BL/6 mice, and GAD67–GFP (neo) knock-in mice from 15 to 20 d of age. The rats were deeply anesthetized by sodium pentobarbital (50 mg/kg) and perfused transcardially with ice-cold sucrose–artificial CSF (ACSF) solution saturated with ox-

Received May 5, 2010; revised Oct. 15, 2010; accepted Oct. 29, 2010.

This research was supported by the National Institutes of Health Grant EY08233 (W.C.H.) and Human Frontier Science Program/Ministry of Education, Culture, Sports, Science, and Technology of Japan Grants 13854029, 18019007, and 18200027 (T.I.) and 20019010 (Y.Y.) and Takeda Science Foundation (Y.Y.). We thank Prof. Young Truong for his assistance with the statistical analysis.

*P.P. and F.M. contributed equally to this work.

Correspondence should be addressed to William C. Hall, Department of Neurobiology, Duke University Medical Center, 327D Bryan Research Building, Box 3029, Durham, NC 27710. E-mail: wch@neuro.duke.edu.

DOI:10.1523/JNEUROSCI.2305-10.2011

 0270-6474/11/311949-06$15.00/0

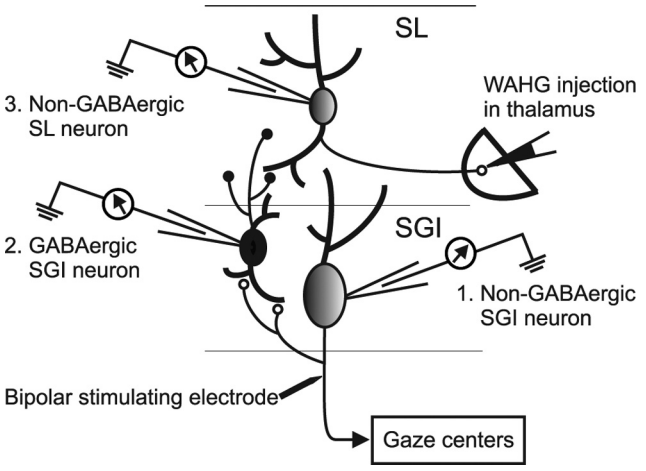

Figure 1. Experimental paradigm to test the circuit model. Antidromic electrical stimulation of the SGI premotor cells was produced by applying pulse currents through bipolar multielectrodes placed ventral to the superior colliculus. Three different types of evoked responses are predicted by the model: (1) antidromically activated action currents in non-GABAergic projection neurons in SGI, (2) monosynaptic or polysynaptic EPSCs in SGI GABAergic neurons that project to SL, and (3) polysynaptic IPSCs in non-GABAergic SL neurons that are retrogradely labeled from the visual thalamus.

ygen. The mice were deeply anesthetized with isoflurane and decapitated. In both groups, the brains were quickly removed and submerged in sucrose–ACSF solution. Slices were cut with a microslicer and then collected in an interface or submersion chamber in standard oxygenated ACSF solution at room temperature for >1 h before recording. The ACSF solution contained the following (in mM): 125 NaCl, 2.5 KCl, 1.25 NaH_2PO_4, 10 $MgSO_4$, 0.5 $CaCl_2$, 26 $NaHCO_3$, and 11 glucose, pH 7.4. Sucrose–ACSF consisted of the same ingredients as the standard ACSF with 200 mM sucrose replacing NaCl.

Prelabeling SL projection cells. To identify SL cells that project to structures outside of SL, in some rats, neurons were prelabeled with the retrograde axonal tracer wheat germ agglutinin–apo–HRP–gold (WAHG) (E-Y Laboratories) before the *in vitro* experiments. Because a major pathway from SL terminates in the dorsal lateral geniculate (dLGN) and lateral posterior thalamic (LP) nuclei of the visual thalamus (May, 2006), WAHG was injected into this region 3–5 d before the patch-clamp experiments. The WAHG is visible with bright-field optics, so the patch-clamp pipette could be guided under direct visual control to the prelabeled cells.

All surgical procedures for these experiments were approved by the Duke University Institutional Animal Care and Use Committee. Animals were deeply anesthetized with a mixture of ketamine (60 mg/kg) and xylazine (10 mg/ kg). Single or multiple injections of 0.1- 0.5 μl of WAHG were delivered stereotaxically into dLGN and LP using a modified Hamilton syringe tip to prelabel SL projection cells by retrograde axonal transport. Animals recovered from the surgery under intensive care and then were returned to their cages until they were used for the slice recordings.

In vitro *whole-cell patch-clamp recording.* Slices were mounted in a recording chamber on an upright microscope and continuously perfused with the oxygenated standard ACSF solution at a flow rate of 2–5 ml/min. Whole-cell patch-clamp recordings were obtained from SL and SGI neurons by visually guiding the patch-clamp pipettes toward identified neurons. GFP-positive GABAergic neurons and GFP-negative neurons were selected from GAD67 knock-in mice using fluorescent optics; then a whole-cell configuration was obtained using bright-field optics. Prelabeled SL projection neurons were identified using bright-field optics, with which the gold appears in the somas as black dots (see Fig. 4*A*).

Patch-clamp pipettes were prepared from borosilicate glass capillaries and filled with a potassium gluconate internal solution for rats or a cesium gluconate internal solution for mice. A potassium gluconate internal solution contained the following (in mM): 130 K-gluconate, 2 Na-gluconate, 20 HEPES, 4 $MgCl_2$, 4 Na_2ATP, 0.4 NaGTP, and 1 EGTA, pH 7.3. Cesium gluconate internal solution contained the following (in mM): 120 CsOH, 10 EGTA, 2 $MgCl_2$.6H2O, 2 Na_2ATP, 10 HEPES, 0.3 Na_3GTP, and 0.1 spermine, pH 7.3. To characterize the morphology of the recorded neurons, biocytin (5 mg/ml; Sigma) was dissolved in the pipette internal solution and allowed to diffuse into the patch-clamped cell. In some experiments, QX-314 [2(triethylamino)-*N*-(2,6-dimethylphenyl) acetamine] (2.5 mM; Sigma) was added to the intracellular solution to block Na^+/K^+ action potentials. With the QX-314, cells could be stably voltage clamped without generating spikes at depolarized potentials to accentuate IPSCs and attenuate EPSCs that may otherwise mask the inhibitory currents.

The resistance of the electrodes was 3.7–9 MΩ in ACSF solutions. The actual membrane potentials were corrected by the liquid junction potential of −10 mV. The neurons were clamped either near their resting membrane potential (−55 to −65 mV) or at depolarized potentials (−30 mV). The whole-cell recordings were performed using a patch-clamp amplifier [Axopatch 1D (Molecular Devices) and EPC-7 (HEKA)] connected through a Digidata 1320A and 1322A analog/digital interface (Molecular Devices). The data were acquired using a pClamp system (pClamp 8.0; Molecular Devices).

Three electrodes from an array of five stainless steel cathodal concentric bipolar electrodes with a tip distance of 200–300 μm (NB Labs and Inter Medical) were used to stimulate the SGI premotor cell axons as they depart the superior colliculus ventral to its deep layers. One of the three electrodes was placed in the lateral midbrain tegmentum, one in the descending tectal efferent fiber tract and one more medially, in the central gray. The stimuli consisted of single cathodal square-wave pulses 100–500 μs in duration with an intensity ranging from 50 μA to 1 mA or 200 Hz of four pulses at 100–700 μA. When synaptic responses were evoked in SGI and SL cells by antidromically activating the SGI premotor cells, the responsible neurotransmitters and their receptors were identified by adding to the slice bath the AMPA/kainate receptor antagonist 6-cyano-7-nitroquinoxaline-2,3-dione (CNQX) (10 μM; Tocris Cookson), the NMDA receptor antagonist DL-2-amino-5-phosphonovaleric acid (APV) (50 μM; Sigma), or the $GABA_A$ receptor antagonist GABAzine/SR95531 [2-(3-carboxypropyl)-3-amino-6-(4-methoxyphenyl)pyridazinium bromide] (10 μM; Sigma) .

Histological procedures. After recording, slices were fixed and stored in 4% phosphate-buffered formaldehyde at 4°C until the slices were processed to visualize the biocytin that had diffused into the neurons from the patch-clamp pipette (Lee et al., 1997; Isa et al., 1998). Briefly, the sections were incubated in 10% methanol and 0.03% H_2O_2 in PBS, followed by 1% Triton X-100 in PBS, and they were freeze-thawed in 20% DMSO. The sections were then incubated in avidin with 0.1% Triton X-100, followed by incubation in biotinylated HRP. Finally, the sections were reacted with 3,3-diaminobenzidine intensified with cobalt and nickel (Adams, 1981). The biocytin confirmed the location of the cell and provided details about its morphology and axonal projections.

Data analysis. Three to eight sweeps of intracellular responses from each stimulation protocol were averaged by using pClampfit 10.2 software (Molecular Devices). Values are given as the means ± SD. Statistical significance was examined with a two-tailed Student's paired *t* test, and the difference was considered significant if $p < 0.05$. We used ANOVA and Tukey's multiple comparisons of means with a 95% familywise confidence level for analysis of differences in response latency among cell groups.

Results

The model predicts that activation of the SGI premotor cells by stimulation of their axons should evoke antidromic spikes in the premotor cells, either monosynaptic or polysynaptic EPSPs in neighboring SGI GABAergic cells, and polysynaptic IPSCs in SL projection cells (Fig. 1).

Antidromic activation of non-GABAergic premotor cells

We tested 12 SGI cells in mice for antidromic activation. The cells were chosen for recording because their size (13–20 μm diame-

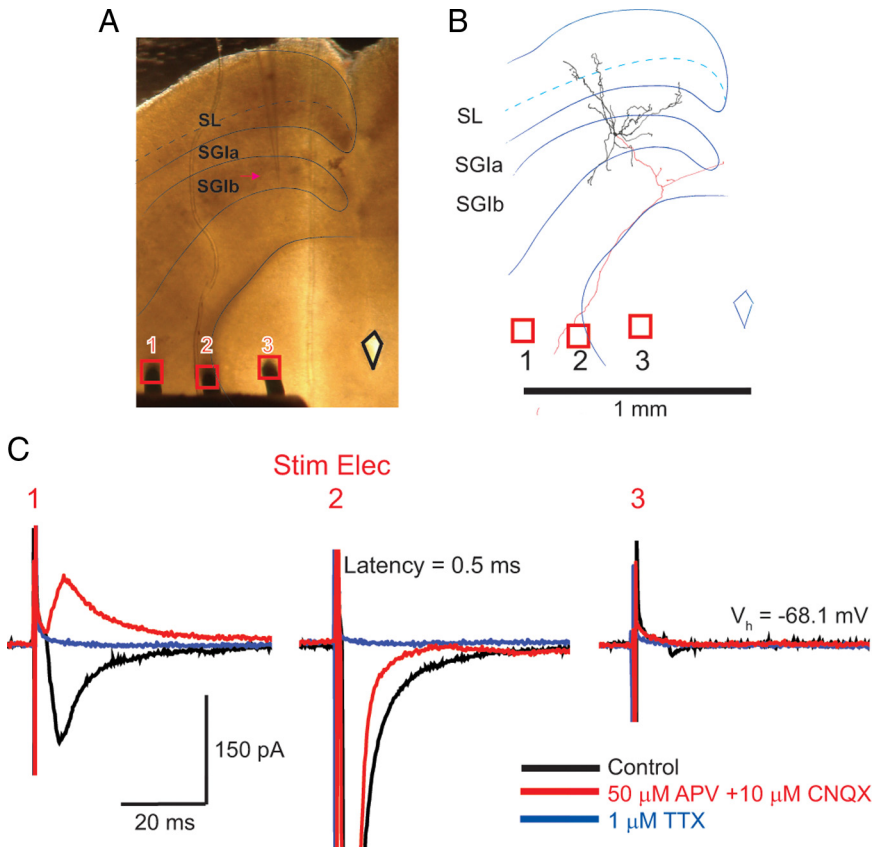

Figure 2. Antidromic activation of a projection neuron in mouse SGI. ***A***, Microphotograph of the slice in which the position of the recorded cell is indicated by a red arrow in SGIb; stimulation electrode sites 1–3 are shown as red squares. ***B***, The biocytin-stained SGI non-GABAergic projection neuron is shown on the slice outline. The axon exits SGI ventrally, in which it passed close to stimulation site 2. ***C***, Responses of the neuron shown in ***A*** to stimulation at sites 1–3. Site 1 evoked only synaptic responses. In site 2, an antidromic spike was induced as a large inward current with short latency (black trace), which was resistant to glutamate receptor antagonists (50 μM APV plus 10 μM CNQX; red trace) but completely suppressed by addition of 1 μM TTX (blue trace). Site 3 evoked little or no response.

ter) and multipolar dendrites are characteristic of SGI projection cells with axons that exit the superior colliculus en route to brainstem gaze centers (Moschovakis et al., 1988b; Isa et al.,1998). Four of these cells generated antidromic spikes, which is consistent with the expectation that only a small proportion of the efferent axons exit SGI in a particular slice. An example of one of these cells is illustrated in Figure 2. Figure 2*A* shows the slice and the location of the stimulating electrodes. Electrode 1 is in the midbrain tegmentum lateral to the main concentration of SGI efferent axons, electrode 2 is centered on these axons as the efferent tract curves around the lateral border of the central gray matter, and electrode 3 is within the central gray, medial to the majority of axons in the efferent tract. A camera lucida drawing of the patch-clamped cell, which was filled with biocytin to reveal its morphology, is superimposed on the slice in Figure 2*B*. The soma of the cell is located in SGI, and its axon leaves the superior colliculus ventrally, in which it intersects electrode 2.

The evoked responses recorded from this cell are illustrated in Figure 2*C*. Electrode 1 evokes synaptic responses in the cell indicating that either cell somas or axons of passage located in the lateral tegmentum project to SGI. The addition of the glutamatergic receptor blockers APV and CNQX reveal an IPSC (red trace) indicating that the response (control) includes both synaptically mediated excitatory and inhibitory components from sources in the lateral tegmentum but no antidromic responses, indicating that this region is not a major destination of axons arising in SGI. The addition of the voltage-gated Na^+ channel blocker TTX to the slice bath to block Na^+/K^+ action potentials eliminates all of the responses, confirming that the currents were evoked by axons that synapse on the voltage-clamped cell and were not a result of non-neuronal electrical spread from the stimulation site. Electrode 2, which is located where the SGI efferent axons congregate, evokes a large, short-latency inward current (0.51 ± 0.11 ms, $n = 4$). The inward current is only slightly reduced by the glutamate receptor blockers, indicating that it is primarily an antidromic response rather than synaptically mediated. TTX confirms that the response is neuronally mediated and not attributable to current spread from the stimulation site. The slight depression of the later part of the inward current by the glutamate receptor blockers suggests that the same stimulation also could activate autapses of the SGI axons or afferent projections to the SGI neurons that passed near the stimulating electrode. Electrode 3, which is more medial in the central gray, fails to evoke either synaptic or antidromic responses, indicating that this region neither sends output to nor receives input from the cell in SGI.

Synaptic activation of GABAergic cells in SGI

GABAergic cells in SGI were identified by their expression of GFP in GAD67–GFP knock-in mice. Of 65 tested cells, 30 generated EPSCs in response to stimulation of the SGI efferent axons. This number is probably a low estimate of the percentage of GABAergic SGI cells that receive input from the efferent axons because some of these connections must be eliminated by the slicing process. In all 30 of the cells that did respond, the EPSCs were blocked by APV/CNQX, indicating that they were synaptic responses mediated by glutamate receptors. Reconstructions of 28 biocytin-filled cells showed that at least six of them had projections to SL.

The responses of a GABAergic SGI cell to antidromic stimulation of the premotor cells are illustrated in Figure 3*A*. The response to stimulation by electrode 1, which again is located in the lateral tegmentum, consists of EPSCs (control; black trace) that are partially reduced by APV (blue) and then completely eliminated by the further addition of CNQX (red). Electrode 2, which is positioned over the SGI efferent axons, evokes EPSCs (control) that are unaffected by APV but completely eliminated by the CNQX. Electrode 3 within the central gray did not evoke a response. Figure 3*B* shows that, as the intensity of the stimulation increases, EPSC amplitude also increases but the latency remains constant, as would be expected for a monosynaptic response. Figure 3*C* shows the distribution of latencies of the EPSCs evoked in the 30 SGI GABAergic cells. The latency distribution has two modes, at 2–3 and 5 ms (mean latency is 3.52 ± 1.29 ms, $n = 30$). The small variation in the latencies of the responses over individ-

ual stimuli (<0.1 ms) also is consistent with a monosynaptic connection between the SGI efferent and GABAergic cells. The less frequent responses with longer latencies are most easily explained by the expected activation of polysynaptic pathways. Figure 3*D* shows the location and morphology of three of these GABAergic SGI cells. Each has a soma in SGI and a prominent axonal projection to SL.

Synaptic inhibition of cells in SL

IPSCs were evoked by antidromic stimulation of the SGI efferent cells in 15 non-GABAergic cells in the SL of mice and in 19 SL cells in rats. Three of these SL cells in rats were identified as projection cells by prelabeling them by the transport of WAHG from the visual thalamus.

In the rats, the peak amplitude of the IPSCs was 154.68 ± 18.46 pA ($n = 19$). The reduction of these IPSCs by APV and CNQX was 32.29 ± 2.66% ($p < 0.001$) and 39.86 ± 2.58% ($p < 0.001$), respectively. The remaining 28% was probably attributable to activation of alternative inhibitory pathways to these cells. In the mice, to minimize activation of other pathways, the stimulus intensity was reduced to the threshold for evoking the IPSCs. In these animals, the peak amplitude of the evoked IPSCs in the non-GABAergic SL cells was 39.86 ± 16.20 pA ($n = 15$). Of these cells, the IPSCs of 13 cells were almost completely blocked by the addition of APV and CNQX to 0.90 ± 2.60 pA ($p < 0.0001$). For the remaining two cells, the IPSCs were partially reduced to 31.64 pA (45.13%) and 41.29 pA (27.05%), respectively.

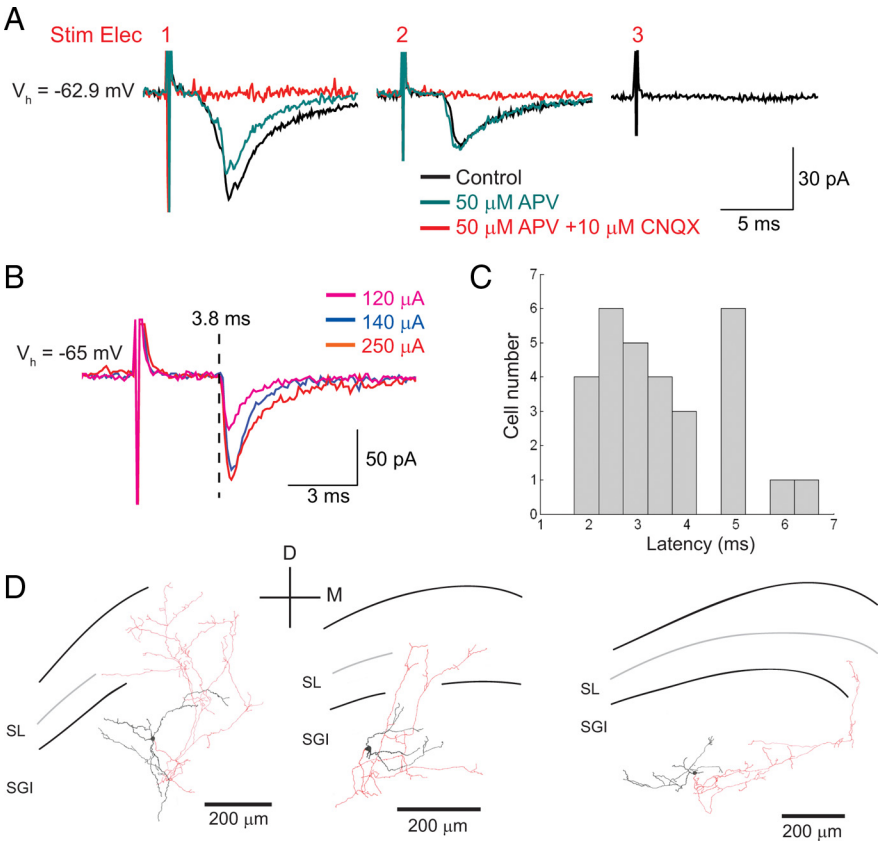

Figure 3. SGI efferent bundle stimulation evoked monosynaptic EPSCs in GABAergic neurons in mouse SGI. ***A***, Examples of current responses evoked from electrodes 1–3 at the holding potential of −62.9 mV. Stimulus intensity was 400 μA. ***B***, Recording from another neuron (holding potential at −65 mV) with various stimulus intensities as indicated in the inset. Note the fixed latencies, which are consistent with monosynaptic responses. ***C***, Distribution of latencies of the EPSCs ($n = 30$). Most of the latencies form a distribution with a mode between 2 and 3 ms. The more rare longer-latency responses are consistent with the activation of polysynaptic pathways. ***D***, Reconstructions showing the somatodendritic morphology (black) and axonal trajectories (red) of three biocytin-filled GABAergic neurons in the SGI with axonal projections to the SL. Right is medial (M), and left is lateral. D, Dorsal.

In the mice, for six cells, the onsets of the IPSCs were distinct enough to reliably estimate their latencies. The mean latency for these was 6.08 ± 1.22 ms ($n = 6$). An analysis of these data using Tukey's multiple comparisons of means with a 95% familywise confidence level demonstrates a significance difference between the latencies of the responses of SGI projection and GABAergic neurons ($p < 0.001$) and between the latencies of the responses of SGI GABAergic neurons and SL projection neurons ($p < 0.001$).

Figure 4*A* illustrates the results from an SL cell in the rat that was prelabeled by an injection of WAHG in LP of the thalamus and generated prominent IPSCs in response to antidromic stimulation of the SGI efferent axons. At the top left, a photomicrograph taken of the *in vitro* slice during the experiment shows the cell in contact with the patch-clamp pipette. The arrowheads point to black dots, which are the gold particles transported to the cell from the thalamus. The middle shows a micrograph of the cell after it was processed for biocytin. The cell soma is in SL and the axon (arrowheads) can be seen leaving SL, presumably en route to the thalamus and/or SGI. The responses of this cell to antidromic stimulation of SGI premotor cells are illustrated on the top right. In these experiments, a train of electrical pulses was used because single pulses to the efferent axons might evoke EPSCs that are too small to generate spikes in the GABAergic SGI cells. The IPSCs evoked in the SL cell of this experiment (control; black trace) are blocked by the combination of APV and CNQX (red trace), which is consistent with the argument that the GABAergic cells that evoke the IPSCs in SL are excited by the antidromic activation of the SGI premotor cells.

The results also indicate that the evoked inhibitory responses in these SL cells are mediated by $GABA_A$ receptors. Figure 4*B* shows for another cell the IPSCs in rat SL that were evoked by repetitive stimulation of SGI efferent axons (left, black trace). The responses also were reduced by APV (blue trace) and almost completely eliminated by the further addition of CNQX (red trace). The traces on the right show the recovery of the IPSCs after the APV and CNQX were washed out (gray trace). These IPSCs then were abolished completely by the application of $GABA_A$ receptor blocker GABAzine (green trace). Results similar to those summarized in Figure 4 for rats also were obtained in non-GABAergic SL neurons in mice.

Discussion

The results show that antidromic stimulation of premotor cell axons where they congregate ventral to the superior colliculus evokes EPSCs in SGI GABAergic cells. The EPSCs can be blocked by the glutamate receptor blockers CNQX and APV, showing that they are synaptically mediated by the SGI efferent cells,

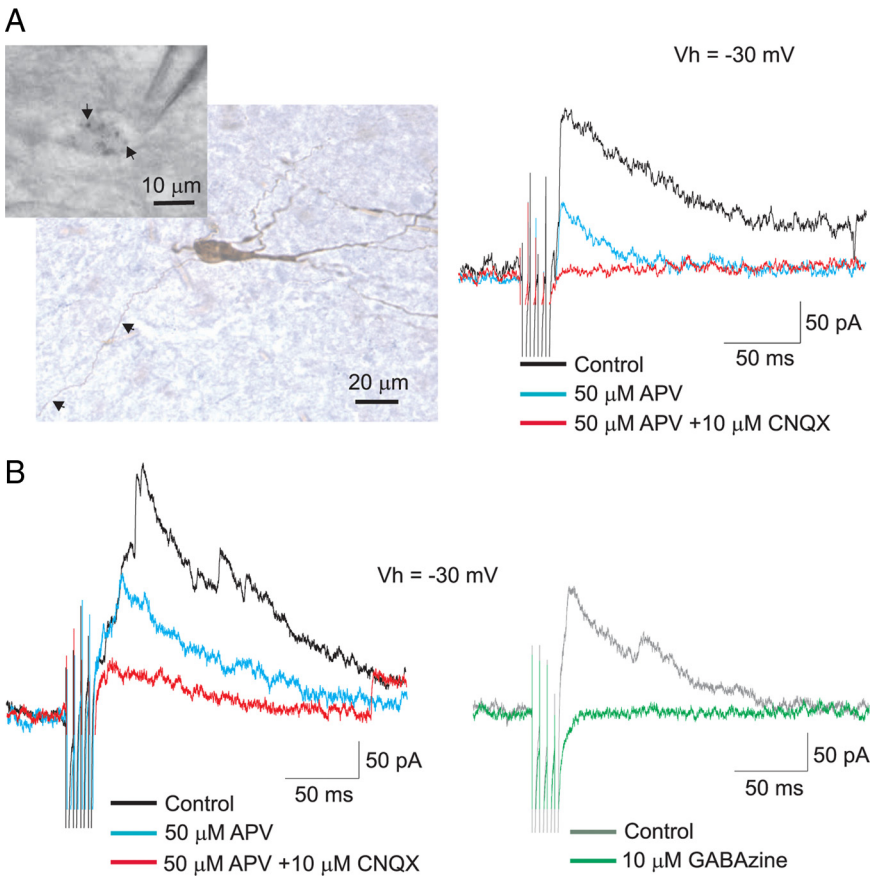

Figure 4. Responses of rat SL cells to antidromic activation of SGI efferent neurons. ***A***, Left, Photomicrograph of a patch pipette in contact with a WAHG prelabeled colliculothalamic neuron in SL. The WAHG appears as black dots (arrowheads) in the cell soma during recording. Middle, Prelabeled colliculothalamic cell revealing the dendrites and axons (arrowheads) that were filled with biocytin. The axon can be traced into the optic layer (arrowheads). Right, The recording in this colliculothalamic neuron shows that antidromic activation of SGI neuron evoked polysynaptic IPSCs (black trace) that were blocked by NMDA and AMPA receptor antagonists (blue and red traces), indicating that an excitatory input activated the GABAergic cells that inhibited the SL cell. ***B***, Left, The evoked polysynaptic IPSCs in another SL cell were mediated by NMDA and AMPA receptors. Right, After washing out NMDA and AMPA antagonists, the evoked IPSCs in SL cell recovered (gray trace) and then were blocked completely by the $GABA_A$ antagonist GABAzine (green trace).

which are known to have local collaterals that terminate within SGI (Moschovakis et al., 1988a; Isa et al., 1998; Lee and Hall, 2006). IPSCs evoked in SL by stimulation at the same site in the efferent bundle were blocked by the $GABA_A$ receptor blocker GABAzine, confirming that the premotor cells in SGI excite GABAergic cells, which inhibit SL cells (Lee et al., 2007).

The circuit model for saccade suppression

The rapid movements of the visual field across the retina during a saccade can be expected to generate retinal activity that, because of conduction time from the retina, reaches the superficial layers of the superior colliculus shortly after the onset of the eye movement and lasts for a short period after the saccade. Saccade suppression refers to the evident attenuation of the influence of this retinal activity on more central visual processing, including visual perception during the saccade and the initiation of subsequent saccades. Experiments designed to identify neural mechanisms responsible for saccadic suppression suggest that neither retinal insensitivity to the rapid saccade induced movement of the visual field nor inhibitory proprioceptive feedback from the extraocular muscles or tendons plays an essential role. For example, extracellular recordings in SL demonstrate that cells can respond vigorously to visual stimuli moving at the velocity of saccades (Goldberg and Wurtz, 1972). Moreover, the suppression of activity in SL can begin before the onset of the saccade and can occur during saccades in the dark, indicating that saccadic suppression is not dependent on reductions in the level of retinal activity during the saccade (Goldberg and Wurtz, 1972). Another hypothesis, that the suppression is mediated by inhibitory input from receptors in extraocular muscles or tendons that detect the eye movements not only is contradicted by the experiments demonstrating that the suppression begins before the onset of the saccade but also by studies that have shown that it occurs when the eyes are paralyzed by retrobulbar injections of lidocaine HCl (Volkmann et al., 1968; Richmond and Wurtz, 1980). In contrast, all of these properties of saccadic suppression are consistent with the circuit model tested in the present paper.

According to the circuit model, the attenuation of activity in the SL neurons, which give rise to a strong projection to SGI (Lee et al., 1997; Isa et al., 1998; Helms et al., 2004; Isa and Hall, 2009), reduces the excitatory input they provide to the premotor output cells during the saccade and thus decreases the likelihood that eye-movement-induced retinal activity will trigger subsequent, unwanted saccades. The excitatory input to the GABAergic cells from the premotor cells might help ensure that the duration of the saccadic suppression in SL approximates the duration of the visual stimulation that occurs as a result of the saccade and also may contribute to the obligatory fixations that occur between successive saccades (Robinson, 1972; Schiller and Stryker, 1972). The SL projection cells also project to the lateral geniculate and lateral posterior nuclei in the dorsal thalamus, both of which are relays to visual areas of the cortex (May, 2006), and the inhibition of this colliculothalamic pathway may contribute to the suppressed perception of the visual field movement that occurs during saccades (Volkmann, 1962; Judge et al., 1980).

Other circuit models for saccade suppression have been proposed, including a pathway from SGI to the intralaminar nuclei that reduces activity in the visual thalamus (Zhu and Lo, 1996), circuits within the cortex (Thiele et al., 2002), and the coordinated activity of widespread neural networks (Kleiser et al., 2004). One model that is especially noteworthy because of its similarity to the current model was proposed by Moschovakis et al. (1988b), in a study that provided evidence for collaterals of SGI premotor cells that ascend to SL. They proposed that these collaterals could contact inhibitory SL interneurons that, in turn, attenuate visual activity during saccades. An alternative possibility consistent with this result is that the ascending collaterals from SGI premotor cells to SL described by Moschovalis et al. (1988b) are spatiotopically organized and excitatory to SL projection cells, and serve to amplify the activity of SL cells in selective regions of the spatial map as part of the process of saccade target

selection. Although the present experiments do not contradict any of these alternative models of the mechanisms underlying saccade suppression, they do provide strong evidence for a circuit that can coordinate a reduction of visual activity in SL with premotor activity in SGI.

References

Adams JC (1981) Heavy metal intensification of DAB-based HRP reaction product. J Histochem Cytochem 29:775.

Goldberg ME, Wurtz RH (1972) Activity of superior colliculus in behaving monkey. I. Visual receptive fields of single neurons. J Neurophysiol 35:542–559.

Harting JK, Hall WC, Diamond IT, Martin GF (1973) Anterograde degeneration study of the superior colliculus in *Tupaia glis*: evidence for a subdivision between superficial and deep layers. J Comp Neurol 148:361–386.

Helms MC, Ozen G, Hall WC (2004) Organization of the intermediate gray layer of the superior colliculus. I. Intrinsic vertical connections. J Neurophysiol 91:1706–1715.

Isa T, Hall WC (2009) Exploring the superior colliculus *in vitro*. J Neurophysiol 102:2581–2593.

Isa T, Endo T, Saito Y (1998) The visuo-motor pathway in the local circuit of the rat superior colliculus. J Neurosci 18:8496–8504.

Judge SJ, Wurtz RH, Richmond BJ (1980) Vision during saccadic eye movements. I. Visual interactions in striate cortex. J Neurophysiol 43:1133–1155.

Kleiser R, Seitz RJ, Krekelberg B (2004) Neural correlates of saccadic suppression in humans. Curr Biol 14:386–390.

Lee P, Hall WC (1995) Interlaminar connections of the superior colliculus in the tree shrew. II. Projections from the superficial gray to the optic layer. Vis Neurosci 12:573–588.

Lee P, Hall WC (2006) An *in vitro* study of horizontal connections in the intermediate layer of the superior colliculus. J Neurosci 26:4763–4768.

Lee PH, Helms MC, Augustine GJ, Hall WC (1997) Role of intrinsic synaptic circuitry in collicular sensorimotor integration. Proc Natl Acad Sci U S A 94:13299–13304.

Lee PH, Sooksawate T, Yanagawa Y, Isa K, Isa T, Hall WC (2007) Identity of a pathway for saccadic suppression. Proc Natl Acad Sci U S A 104:6824–6827.

May PJ (2006) The mammalian superior colliculus: laminar structure and connections. Prog Brain Res 151:321–378.

Moschovakis AK, Karabelas AB, Highstein SM (1988a) Structure-function relationships in the primate superior colliculus. I. Morphological classification of efferent neurons. J Neurophysiol 60:232–262.

Moschovakis AK, Karabelas AB, Highstein SM (1988b) Structure-function relationships in the primate superior colliculus. II. Morphological identity of presaccadic neurons. J Neurophysiol 60:263–302.

Phongphanphanee P, Marino R, Kaneda K, Yanagawa Y, Munoz D, Isa T (2008) The lateral interaction in the superficial and intermediate layers of the mouse superior colliculus slice. Soc Neurosci Abstr 34:167.17.

Richmond BJ, Wurtz RH (1980) Vision during saccadic eye movements. II. A corollary discharge to monkey superior colliculus. J Neurophysiol 43:1156–1167.

Robinson DA (1972) Eye movements evoked by collicular stimulation in the alert monkey. Vision Res 12:1795–1808.

Schiller PH, Stryker M (1972) Single unit recording and stimulation in superior colliculus of the alert monkey. J Neurophysiol 35:915–924.

Tamamaki N, Yanagawa Y, Tomioka R, Miyazaki J, Obata K, Kaneko T (2003) Green fluorescent protein expression and colocalization with calretinin, parvalbumin, and somatostatin in the GAD67-GFP knock-in mouse. J Comp Neurol 467:60–79.

Thiele A, Henning P, Kubischik M, Hoffmann KP (2002) Neural mechanisms of saccadic suppression. Science 295:2460–2462.

Volkmann FC (1962) Vision during voluntary eye movements. J Opt Soc Am 52:571–578.

Volkmann FC, Schick AM, Riggs LA (1968) Time course of visual inhibition during voluntary saccades. J Opt Soc Am 58:562–569.

Zhu JJ, Lo FS (1996) Time course of inhibition induced by a putative saccadic suppression circuit in the dorsal lateral geniculate nucleus of the rabbit. Brain Res Bull 41:281–291.